

ASSESSMENT OF STRUCTURAL STEEL MEMBERS TEMPERATURES IN OPEN CAR PARK FIRES: DIFFERENT MODELLING APPROACHES

Xia Yan¹, Marion Charlier², Thomas Gernay³

ABSTRACT

Open car parks, as defined based on ventilation conditions, are one of the most common types of car park buildings. For such structures, adopting a performance-based structural fire design based on localised fires is often justified and allowed because the fire does not reach flashover. As this approach requires assessing the temperatures in the structure, this paper focuses on the numerical analysis of the temperatures reached in open car park steel beams under localised fires through different approaches. Simple analytical localised fire models and advanced CFD-FEM coupling methods are used to evaluate the beam temperatures. Several parameters are considered and varied: the dimensions of the steel elements, layout of burning vehicles, galvanization of the steel, and the modelling approaches. Results show that the temperatures reached in the investigated steel profiles are influenced by the location and number of burning vehicles; open car park fires generate thermal exposure conditions vastly different from the nominal fires. Galvanization of the steel profiles has the effect of delayed heating and reduced peak temperature under open car park fires. In terms of the modelling approach, Hasemi model is overconservative and gives erroneous results with galvanization, while adopting an advanced CFD-FEM modelling approach shows advantages and benefits for the performance-based design of open car parks in fire conditions.

Keywords: Open car park, localised fire, steel frame, numerical modelling, CFD-FEM.

1 INTRODUCTION

In open car parks, a spatially uniform temperature field does not capture the thermal exposure conditions for the structure. Instead, localised fire models are preferred to simulate burning cars and assess the heating of adjacent structural members. The definition of open car park depends on the country or jurisdiction under consideration [1], and it usually relies on a ratio of openings to surface of the boundaries of enclosure (openings present on opposite façades also have an influence). Modelling of localised fires can either be based on simple models, e.g., the models by Heskestad [2], Hasemi [3], and LOCAFI [4], which have each their field of application; or on advanced numerical modelling such as computational fluid dynamics [5]. In previous studies, the Hasemi model was used to analyse the thermal effect from burning vehicles on a steel beam [6] and to analyse multi-story car parks [7]. In another study, the Hasemi and the LOCAFI models were applied to study the fire performance of a steel open car park subjected to the fire scenario relevant for the columns [8]. While these studies provided insights into the thermal response of structural members in car park fires, no comparison of the temperatures predicted by different modelling approaches were performed, with the exception of a study that suggested that application of the Hasemi model led to

¹ Department of Civil and Systems Engineering, Johns Hopkins University, Baltimore, U.S.A. (now work at Simpson Gumpertz & Heger)
e-mail: xyan18@jhu.edu, ORCID: <https://orcid.org/0000-0002-1263-3417>

² ArcelorMittal Steligenge, Esch-sur-Alzette, Luxembourg
e-mail: marion.charlier@arcelormittal.com, ORCID: <https://orcid.org/0000-0001-7690-1946>

³ Department of Civil and Systems Engineering, Johns Hopkins University, Baltimore, U.S.A.
e-mail: tgernay@jhu.edu, ORCID: <https://orcid.org/0000-0002-3511-9226>

more conservative thermal actions than the FDS-FEM coupling [9]. Further, the effect of steel galvanization on the temperature rise in steel framing members has not been studied in the context of open car park fires, yet galvanization is expected to affect the heat transfer through a reduction of the steel emissivity. This research therefore aims to assess the influence of galvanization when assessing the steel beam temperatures in an open car park, and to perform a systematic comparison of simple and advanced modelling approaches. This study focuses on the analysis of the temperatures reached in open car park steel beams subjected to car fires. Various modelling approaches are adopted to simulate the localised fires. Both simple analytical localised fire models and advanced CFD-FEM (Computational Fluid Dynamics – Finite Elements Method) coupling methods are used. The simple models in this study include the Heskestad [2], Hasemi [3], and LOCAFI [4] models. As each of these models have their own scope of application, the choice made between these models depends on the structural member under consideration (beam or column) and on its relative position from the burning vehicles. For the advanced numerical modelling, the FDS software is adopted with two methods to interface the FDS simulation of the localised fires with the subsequent FEM thermal analysis. The first one uses the concept of Adiabatic Surface Temperature (AST), while the second method, referred to as the FDS-FEM interface, uses a transfer file containing the gas temperatures and radiant intensities from FDS in a format readable by the FEM software. In addition, analyses are carried out to investigate the effects on steel temperatures of parameters including the dimensions of the steel members, the layout of burning vehicles, and galvanization of the steel. The case study considers a medium-sized multi-story open car park with a typical steel-concrete composite structure with steel framing and concrete flat slabs.

2 DEFINITION OF THE CAR PARK LAYOUT

2.1 Steel beams

The study focuses on a medium-sized multi-story open car park [9]. The distance between the floor and the bottom part of the ceiling is 2.5 m. The floor plan of the car park is 60×48 m, with 5×2.5 m standard parking bays. The structure is a steel-concrete composite structure with steel framing and concrete flat slabs. Two members are considered for the beams: a steel hot rolled profile IPE450 (common design in composite steel-concrete car parks for 16 m primary beams spaced 2.5 meters apart), and a steel hot rolled profile HEA600 (common design for 16 m primary beams spaced 5 meters apart) [9]. The dimensions of the profiles are shown in Figure 1. No fire protection is applied to the structure. To study the influence of galvanization on steel temperatures, the analysis is conducted for both ungalvanized profiles and galvanized profiles. Following EN 1993-1-2 [10], the emissivity of ungalvanized steel is taken as 0.7 (value independent of the temperature). The thermal behaviour of the galvanized steel is the same as that of ungalvanized steel except that the emissivity is 0.35 up to first heating to 500 °C, and 0.7 beyond. This is because the zinc coating applied on the surface of the steel irreversibly melts at a temperature of 500 °C.

2.2 Localised fires: burning cars layout

The heat release rate (HRR) for burning vehicles (class 3 cars) is adopted from the CTICM Guidebook for the verification of open car parks subjected to fire [11]. This HRR curve car was obtained from experimental campaigns (more details can be found in [12]). In “Development of design rules for steel structures subjected to natural fires in closed car parks” [12], an experimental campaign which took place in a semi-closed carpark with large dimensions (85x55x3m) is described. The time shift of fire propagation between nearby cars was observed and served as reference for open car park fire design. Thus, the ignition of cars next to the first car igniting the fire is delayed by 12 minutes.

For the heating of the steel beams, three scenarios were considered that involve between one and three burning cars, as shown in Figure 2. In the first scenario, a single car is burning, and it is positioned right below the beam. In the second scenario, a single car is burning, but with an offset from the axis of the beam. This layout is representative of situations where the beam is located above the boundary between two adjacent car park bays. In the third scenario, three cars are burning underneath the beam, which axis is aligned with the middle car.

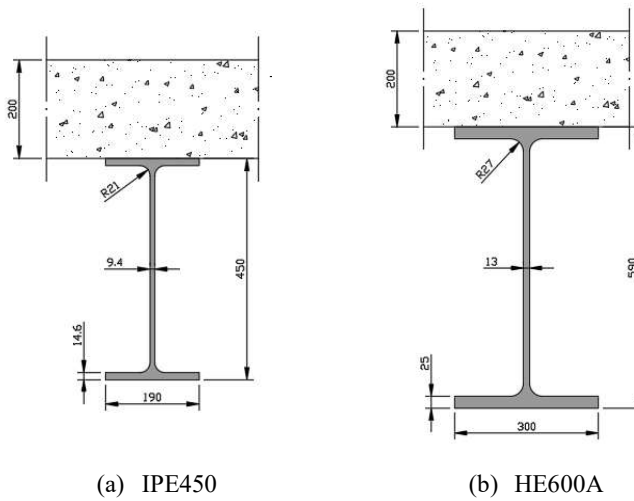


Figure 1. Dimensions of the steel beam profiles (units: mm).

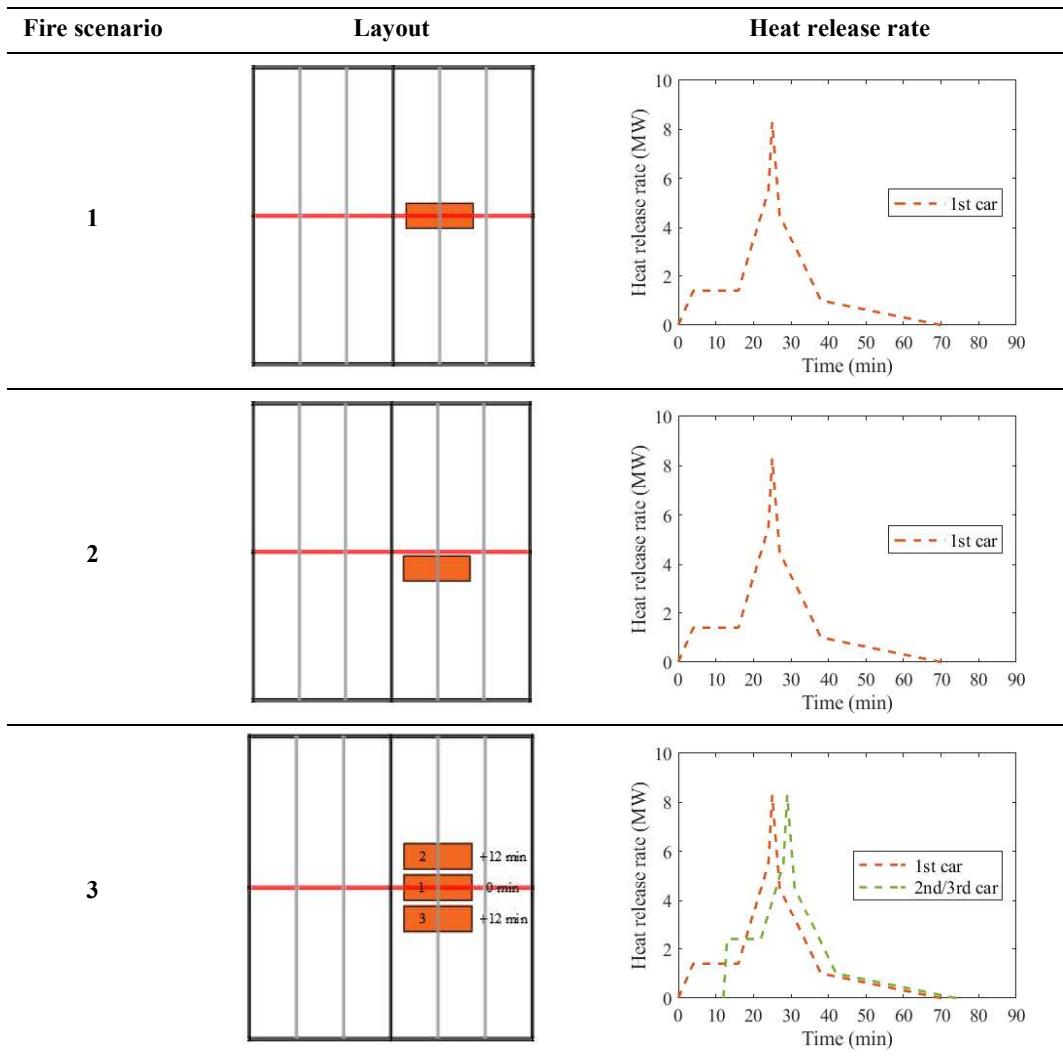


Figure 2. Fire scenarios considered for the modelling of the thermal exposure on steel beams (burning cars are shown in orange, structure of interest is shown in red).

The Guidebook from CTICM [11] recommends a scenario with seven cars placed transversally when studying the fire response of open car park beams. Given that the present study focuses on the heating modelling at a given section, the scenario with seven cars was not further considered. This assumption was validated by localised fire analyses conducted in OZone [13] (in accordance with the Annex C in EN1991-1-2 [14]). Indeed, these analyses allowed to verify that the considered beam temperatures under five burning cars and three burning cars (located transversally in the mid-span cross-section of both the IPE450 and HE600A sections) are similar, as shown on Figure 3. As a result, it can be assumed that peak steel temperatures in the beams would not be higher with seven cars transversally than with three cars.

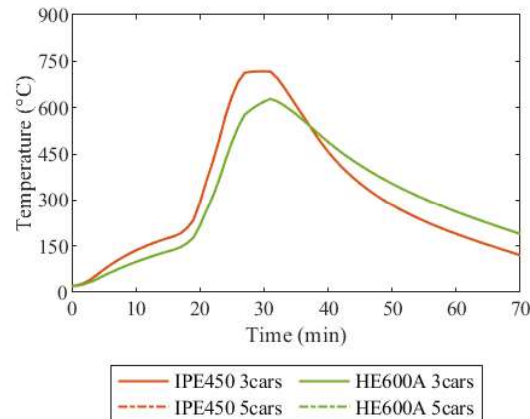


Figure 3. Temperature in IPE450 and HE600A beams when subjected to 3 and 5 burning cars positioned transversally to the beam axis, as calculated with OZone (localised fires). The temperature curves for 3 and 5 cars for a given profile are superposed.

3 THE FIRE MODELLING APPROACHES

3.1 Application domain

Both simple models and advanced modelling approaches are available for simulating member temperatures under localised fires. Benchmarking against test data is provided in a recent study by the authors [15]. The main features of the models are summarized hereafter.

The simple modelling approaches for localised fires include the Heskestad, Hasemi, and LOCAFI models. The Heskestad model is used to evaluate the flame temperature along the vertical centreline of the fire when the flame is not impacting the ceiling (e.g., for columns coinciding with the centreline of the fire or for part of the beam located just above the fire). The Hasemi model evaluates the heat flux received by the unit surface area at the ceiling level when the flame touches the ceiling (e.g., for beams or for column tops). The LOCAFI model calculates the radiative heat flux received by a vertical member not engulfed in the fire area (e.g., a column). As these models have different scopes of application, the selection of the applicable simple model results from the situation which is under consideration.

Advanced numerical modelling approaches rely on CFD to simulate the localised fire. A commonly used tool is FDS [5]. There are two main approaches to interface a FDS simulation with a subsequent FEM thermal analysis. The first uses the concept of Adiabatic Surface Temperature (AST) to transfer the thermal boundary information [16]. It assumes the surface to be a perfect insulator and the net heat flux is thus zero. The fictitious temperature T_{AST} is calculated based on the incident radiative heat flux and the gas temperature near the surface [17]. Then the T_{AST} is applied to the FEM thermal analysis as thermal boundary condition. This method is referred to as the FDS-FEM AST method. The second method is referred to as the FDS-FEM interface method. It uses a transfer file containing the gas temperature and radiant intensities in the field of interest in FDS in a format readable by the FEM software [9]. Then the transfer file is processed by the FEM software that interprets the quantities in terms of thermal boundary conditions [18].

Figure 4 shows the applicable fire models based on the configuration between the localised fire and the steel member. The study focuses on beams. When using simple models for analysing beam sections outside the fire area (section ‘B1’ and ‘B2’), the heat flux should be taken from the Hasemi model. However, if beam sections are inside the fire area (section ‘B3’), the heat flux should be taken as the maximum between the Hasemi flux and the flux computed based on the flame temperature from the Heskestad model. When selecting CFD-based modelling approaches, the FDS-FEM AST method is applicable to all configurations. The structural frame members should be included in the FDS model when adopting the AST method. The FDS-FEM interface method is applicable for structural members that are far from the fire source (section ‘B1’); the relevant distance being such that the presence of the structural members does not noticeably affect the continuity of the temperature and radiative fields. These frame members should be omitted in the FDS model when using the interface method [15]. The ability to omit the frame members from the FDS simulation and to rely on an automatic transfer file between FDS and a FEM software is advantageous in terms of modelling effort. For sections closer to the heat source, which significantly influence the mass flow or radiative flow in the compartment (section ‘B2’), the frame members should be included in the FDS model and the AST method is preferred for the transfer of thermal information; except if the section is right above the heat source (section ‘B3’), in which case owing to symmetry both FDS-FEM AST and FDS-FEM interface methods are applicable.

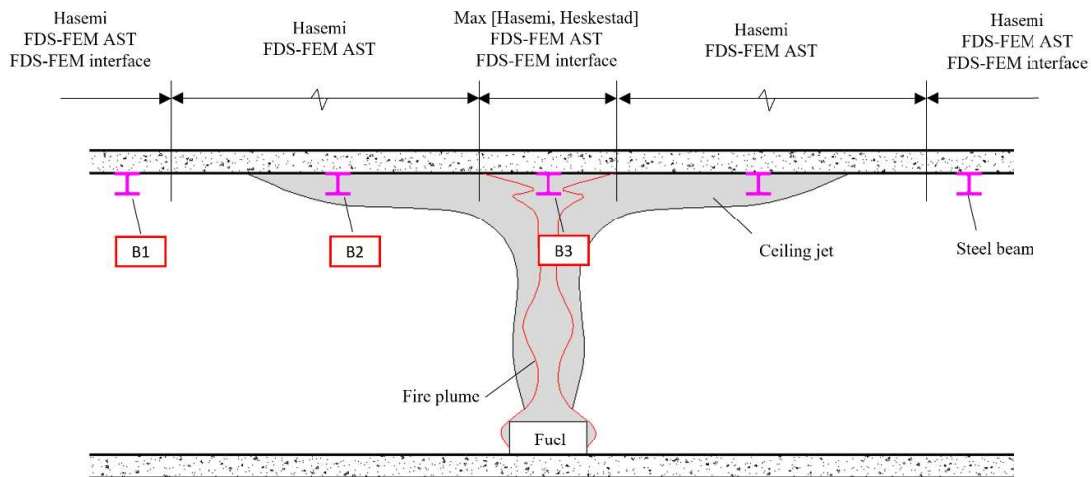


Figure 4. Application domain of localised fire modelling approaches for localised fires (not to scale).

3.2 CFD simulations and analytical models: fire development

The Fire Dynamics Simulator (FDS, version 6.7.1) is adopted to run the CFD simulations. The computational domain in FDS is $30 \times 22.5 \times 3$ m (length \times width \times height) for the simulations of fire scenarios. A sensitivity analysis was conducted on the computation domain to minimize the border effects with respect to the smoke flow. Burning cars are modelled as rectangular blocks with dimension of $4.8 \times 1.8 \times 0.3$ m each. The heat release rate of the burning car is taken as the heat flux curves in Figure 2. Based on research for car fires, the soot yield is set to 0.22 [19], and heat of combustion is set to 44.4 MJ/kg, typical of gasoline [9]. A mesh size of $0.1 \times 0.2 \times 0.1$ m is selected. The special resolution $R^* = dx/D^*$, where dx is the characteristic length of a cell for a given grid and D^* is the characteristic diameter of a plume, calculated with the selected mesh size falls into a reasonable range of $1/10 \sim 1/20$ [5].

The fire development is also investigated with the simple models described above. The burning car is modelled as a 3.2 m-diameter circular plan area with equivalent fire area for a typical car park spot. The axis of the localised fire is at the center of car. The heat release rate of the burning car is consistent with the heat flux curves in Figure 2.

3.3 FEM simulations: heat transfer to the steel beams

The heat transfer analysis to the steel member is conducted with the FEM software SAFIR [21]. SAFIR allows applying thermal boundary conditions to the surfaces of the steel members which are imported from

FDS simulations or from the simple localised fire models provided in the Eurocodes, i.e., Hasemi, Heskestad, and LOCAFI (i.e., solid flame) [20]. A series of 2D thermal analyses are conducted at each longitudinal integration point of the structural member. Thermal analysis of the cross section is carried out using solid conductive elements and capturing the convection and radiation at the boundaries. The equations to capture radiative and convective heat flux to the steel member are in accordance with the Eurocode EN1991-1-2 [14] and are detailed in [21]. Longitudinal variations in temperature distributions are captured by analysing several cross-sections along the beam length; heat transfer in the longitudinal direction of the steel beam and column is neglected as the longitudinal dimension of the member is order of magnitudes larger than the thickness of the plates.

The steel member is included in the FDS analysis when using the AST method. 14 sensors are attached onto the structural surface of cross sections at an interval of 0.2 m in the longitudinal direction to measure the AST. Then, the AST outputs from FDS are applied onto the SAFIR 2D thermal model as boundary condition (temperature-time Frontier constraint). For the interface method, the structural member is not included in the FDS model. The gas temperature and radiant intensities are output from FDS at the grids surrounding the structural member with a time step of 10 seconds and written into a transfer file. The transfer file is applied onto the SAFIR 2D thermal model as thermal boundary condition (Flux constraint).

When the fire development is computed through analytical models, different flux constraints are available in SAFIR. The flux constraint ‘Hasemi’ computes the flux applied to each point of integration of the steel beams based on the simple Hasemi model, for situations where the localised fire flame is touching the ceiling. For columns not engulfed into the fire, the LOCAFI model can be applied. SAFIR then evaluates the flux using the solid flame model, assuming that the burning car is represented by a cone shape fire. For members in the axis of the flame (columns and beams, if the localised fire flame is not touching the ceiling), the Heskestad model is applied, as depicted on Figure 4. The equations from Eurocode EN1991-1-2 are used to evaluate the flame temperature along the vertical axis of the fire. The heat flux to the member is then evaluated considering both the convective and radiative heat flux. It is worth noting that the Heskestad model is embedded in the flux constraint named ‘LOCAFI’ in SAFIR. With the flux constraint ‘LOCAFI’ applied, the heat transfer computation in SAFIR automatically shifts between the virtual solid flame model and the Heskestad model considering the relative position of the point of integration and the fire flame. When the point of integration (POI) is in the flame, a convective flux with the flame temperature and radiative heat flux with this temperature and a view factor of 1 are considered. The flame temperature is calculated by the Heskestad model in the centreline of the flame at the height of the POI. When the POI is located outside the flame, only the radiative heat flux is considered with the LOCAFI model.

The thermal properties of the steel are in accordance with Eurocode EN1993-1-2 [10]. The conductivity and specific heat vary with the temperature. The convection coefficient is taken as 35 W/m²K, in accordance with Eurocode EN1991-1-2 for natural fire exposures [14]. The emissivity of the ungalvanized profiles is taken as $\epsilon = 0.7$, while for the galvanized profiles, a newly developed material named GALVASTEEL is implemented in SAFIR: it is such that $\epsilon = 0.35$ up to 500 °C and then $\epsilon = 0.7$ beyond that. A mesh size of 0.01 m is adopted for all the thermal analyses (see Figure 5 (a) and (b)).

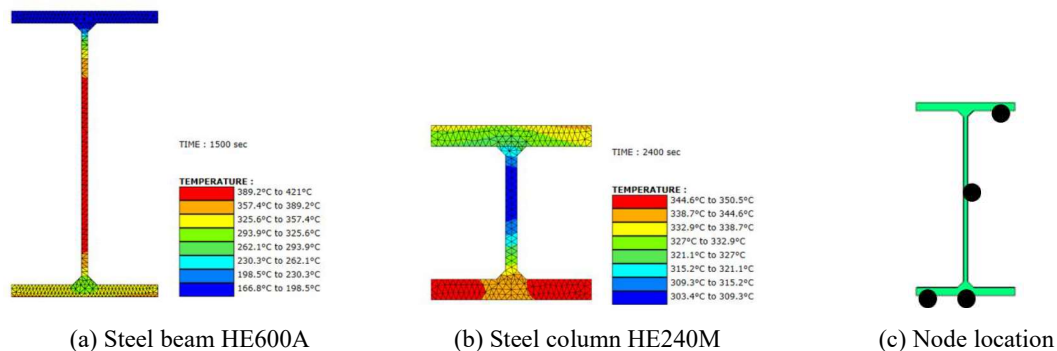


Figure 5. Finite element mesh for the thermal analysis of (a) HE600A, (b) HE240M, and (c) location of the nodes used to compute average steel temperatures.

4 TEMPERATURE DEVELOPMENT IN THE BEAMS

4.1 Fire Scenario 1

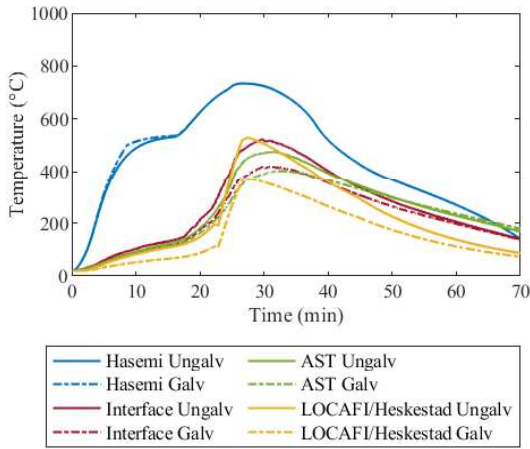
Localised fire scenario 1 includes a single burning car directly underneath the beam (Figure 2). The steel beam temperatures at the lower flange of the mid-span cross section are plotted in Figure 6 (a) and (b). Solid and dashed lines are used for the ungalvanized and galvanized profiles, respectively. The two FDS-FEM methods yield similar results for the IPE450 profile, while the interface method is slightly more conservative than the AST method for the HE600A profile. This verifies that for the structures located at the ceiling level and right above the heat source, the interface method is applicable, as shown in Figure 4 B3. In the FDS interface simulation, the beam is not modelled in FDS, but the flat slab ceiling is. When comparing the member temperatures reached in different profiles, the IPE450 experiences temperatures higher by almost 120 °C than HE600A due to the higher section factor.

Galvanization reduces the emissivity and hence the amount of heat transferred into the section. Both the AST method and interface method indeed predict reduced temperatures when the profile is galvanized. The peak temperature is reduced by 53 °C in the web and 69 °C in the flange of IPE450 at the center section. As for the HE600A profile, the peak temperature is reduced by 68 °C in the web and 73 °C in the flange at the center section. The time to reach the peak temperature is also delayed by about 1 minute for IPE450 and 2 minutes for HE600A due to galvanization.

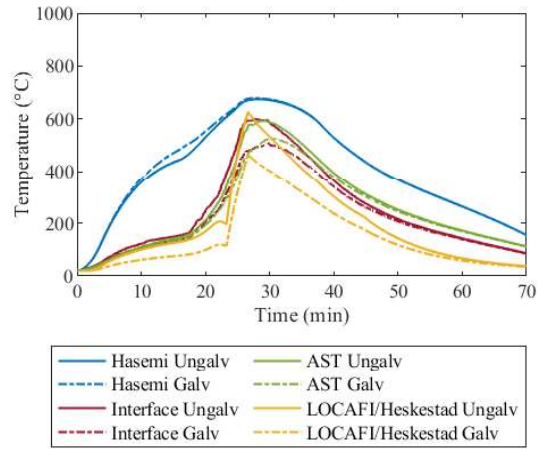
Results are also given for simple models of localised fires. For the configuration of scenario 1, two analyses are completed. The first is with the Hasemi model. Strictly speaking, the Hasemi model only applies when the flame touches the ceiling, while in the early stage of the fire this is not the case. Evaluating the heat flux throughout the localised fire event with the Hasemi model (“Hasemi” flux boundary condition in SAFIR) is thus expected to yield conservative results. Another approach is to evaluate the flux based on the flame temperature from the Heskestad model. This second approach (“LOCAFI” flux boundary condition in SAFIR) evaluates the flame temperature along the vertical axis of the fire, then applies either the virtual solid flame model to compute radiative flux to the beam at the early stage of the fire when it is outside the flame or computes the convective and radiative flux to the beam once it is inside the flame. In this second approach, the FE software automatically transitions from the former flux computation to the latter based on the flame height. To indicate that both LOCAFI and Heskestad models are combined in this second approach, the curves in Figure 6 are labelled as LOCAFI/Heskestad.

The Hasemi model significantly overestimates the steel temperatures, compared to the FDS-FEM AST/interface method. The overestimation is greatest during the initial heating phase. At 15 min, the temperature difference between the Hasemi model and AST method reaches 420 °C in the lower flange of the ungalvanized HE600A profile, as shown in Figure 6 (1). Differences in peak temperatures are also notable; the peak temperature difference between Hasemi model and AST method is 260 °C in the lower flange of ungalvanized HE600A profile. Another issue with the Hasemi model is that it erroneously represents the influence of galvanization on the member temperature. Contrary to the observation with FDS-FEM, Hasemi yields slightly higher steel temperature in the galvanized profile compared with the ungalvanized one. The causes for these shortcomings of the Hasemi model are discussed in Section 4.3.

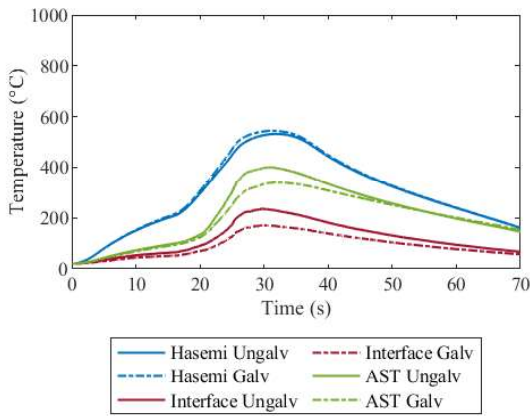
Regarding the LOCAFI/Heskestad model (“LOCAFI” flux boundary condition in SAFIR), during the initial stage when the HRR from the burning car is small and the analysed section is outside the flame, lower temperatures are obtained compared with the FDS-FEM AST method. In this initial stage, the flux is computed based on the virtual solid flame, hence convection is neglected. After the flame touches the ceiling and the section is inside the flame, both the convective and radiative heat flux are taken into account, evaluated based on the flame temperature from the Heskestad model. The model yields similar estimations of the peak temperatures reached in the profiles as the FDS-FEM AST method. The ability of this implementation of the simple model to transition from virtual solid flame when the member is outside the flame to convection and radiation once the member becomes engulfed is clearly visible in the results, with a sudden increase in temperatures that matches that obtained with FDS. It also captures the influence of galvanization with lower emissivity leading to lower temperature.



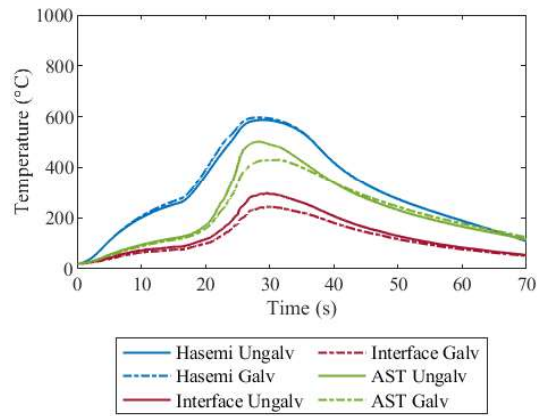
(a) Lower flange of HE600A – Scenario 1



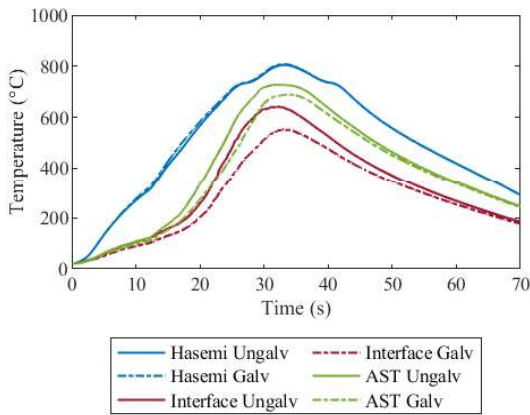
(b) Lower flange of IPE450 – Scenario 1



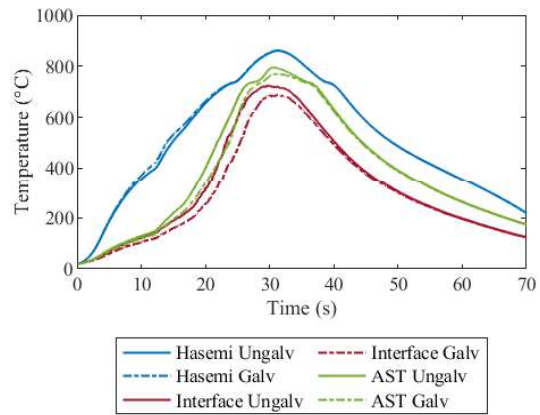
(c) Lower flange of HE600A – Scenario 2



(d) Lower flange of IPE450 – Scenario 2



(e) Lower flange of HE600A – Scenario 3



(f) Lower flange of IPE450 – Scenario 3

Figure 6. Temperature evolution in the lower flange of HE600A and IPE450 profiles under the three scenarios.

4.2 Fire Scenarios 2 and 3

The steel beam temperatures at the mid-span cross section obtained from various methods under localised fire scenarios 2 and 3 are shown in Figure 6 (c) to (f). The FDS-FEM interface method yields lower member temperatures than the FDS-FEM AST method, especially at the lower flange. It is worth noting that the steel beam is not modelled in FDS with the interface method. Omitting the beam is necessary to avoid unwanted averaging effects in the spatial integration of the temperature and flux fields by the FEM as shown in [15]. However, this means the impact of the presence of structural member on the fire development is neglected. The discrepancy in terms of the member temperature obtained with the FDS-FEM AST and interface method indicates that when the section is not right above the heat source, the influence of the presence of the structural member should not be neglected. Thus, the interface method is not recommended for this situation. Due to galvanization, the peak temperature is reduced by more than 60 °C for HE600A and IPE450 profiles in fire scenario 2.

In fire scenario 3, the galvanization has less dominant effect on the peak temperature due to the more intense heating. The peak temperatures reached in fire scenario 2 are lower than those reached in fire scenario 1 due to the offset of the beam, while the peak temperatures reached in fire scenario 3 are higher than those reached in fire scenario 1 due to the higher heat release rate when three cars are burning instead of one. When comparing the member temperatures in different profiles, IPE450 experiences temperatures about 60 °C to 100 °C higher than the HE600A due to the different section factor.

The Hasemi model again overestimates the member temperatures compared with the FDS-FEM AST method. It is on the conservative side, with discrepancies not as large as for scenario 1, but still possibly making it overconservative for design. As observed previously, the Hasemi model also yields erroneous results on the effect of galvanization, because it cannot correctly capture the effect of a change in emissivity on the absorbed heat flux (See Section 4.3).

The peak temperatures obtained from the FDS-FEM AST method are summarized in Table 1. The listed values are obtained at the time of peak temperature in the profile and are the average of the temperatures at the bottom of lower flange, center of lower flange, mid web, and bottom of upper flange, as shown in Figure 5 (c). When subject to open car park fires, galvanization has the effect of delayed heating and reduced peak temperature. As listed in Table 1, the peak temperatures in HE600A are reduced by more than 60 °C and those in IPE450 are reduced by more than 50 °C under localised fire scenarios 1 and 2 when galvanization is applied to the steel members. The influence of galvanization on reduced peak temperature is less dominant in localised fire scenarios 3, see Figure 6. This is because the zinc coating applied on the surface of the steel melts at a temperature of 500 °C, so the member temperatures gradually catch up with the fire temperature for severe fire exposures.

4.3 Limitations linked to the use of Hasemi model

It was shown that the Hasemi model leads to higher predicted steel temperatures than the FDS-FEM coupling methods. The main reasons of this noticeable difference are the following:

- (i) The Hasemi model assumes that the flame touches the ceiling. It is an empirical model which flux is calibrated on an experiment during which the flame was touching the ceiling. Figure 7 shows the HRR cloud map captured at different time steps in the FDS simulation of localised fire scenario 1. It can be observed that the flame is not impacting the ceiling (grey block in Figure 7) before 1000 s (growing phase in the HRR curve of class 3 car shown in Figure 2) and after 1900 s (cooling phase) in the FDS simulation. In other words, as can be observed in FDS modelling, the flame touches the ceiling during only one sixth of the whole fire duration.
- (ii) The Hasemi model was derived from experimental tests in which the ceiling was made of perlite boards. The concrete slab in a car park behaves as a heat sink that absorbs a large amount of energy (larger than with perlite boards), which causes a decrease in gas temperature at the ceiling level.
- (iii) The Hasemi model does not capture the shadow effect, i.e., all boundaries of the section receive the same heat flux with the value calculated at the point of integration in FEM software. For open sections with concave parts, the received heat flux evaluated by the Hasemi model is therefore overestimated.

Table 1. Peak temperatures of galvanized and ungalvanized profiles under localised fire scenarios (obtained from FDS-FEM AST method, averaged over the profile section).

Profile	Average temperatures under scenario 1 (°C)	Average temperatures under scenario 2 (°C)	Average temperatures under scenario 3 (°C)
HE600A			
Ungalva	428	355	671
Galva	369	309	628
Difference	59	46	43
IPE450			
Ungalva	551	453	749
Galva	494	397	718
Difference	57	56	31

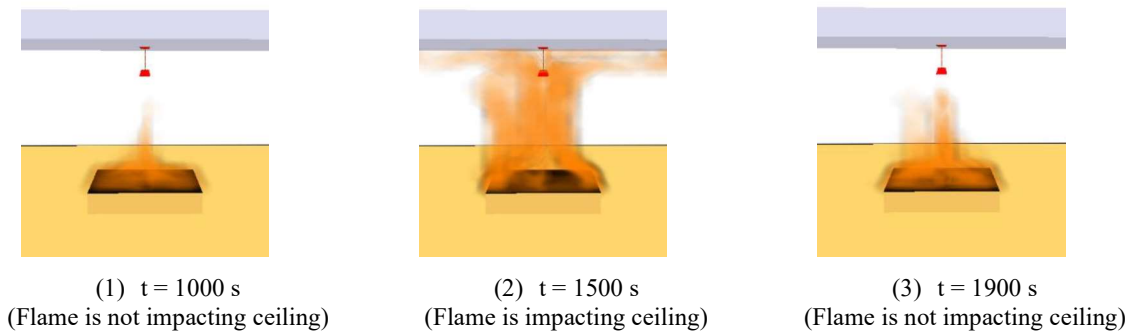


Figure 7. HRR cloud map obtained from FDS simulation of the localised fire scenario 1 shows that the flame does not touch the ceiling (grey block) for most of the fire duration.

Besides, the Hasemi model gives erroneous results when applied to a material with different thermal properties than the ones for which the model was calibrated. More specifically, Hasemi model gives higher member temperatures with lower emissivity. This is because the heat flux given by the Hasemi model is in fact inherently an absorbed heat flux, meaning that it does not depend on the thermal properties of the receiving member (because it is already implicitly multiplied by the thermal properties of the material for which it was calibrated). When using the Hasemi model, the net heat flux on the boundary of a solid is evaluated with Eq. (1).

$$\dot{q}_{net} = \dot{q}_{hasemi} - h_{hot}(T_s - T_{amb}) - \sigma \varepsilon (T_s^4 - T_{amb}^4) \quad (1)$$

where \dot{q}_{hasemi} is the flux computed according to Eq. (C.4) of EN 1991-1-2 [14] (incoming “absorbed” flux from the plume) [10]; h_{hot} is the coefficient of convection on exposed surfaces; T_s is the temperature at the surface of the solid at the boundary; T_{amb} is the ambient temperature; σ is the constant of Stefan Boltzmann; ε is the emissivity of the material of the solid. As can be seen in Eq. 1, the incoming (absorbed) part is independent of the thermal properties of the solid, whereas the outgoing (re-emitted) part depends on h_{hot} and ε . In this study, the steel member is analysed in two configurations: ungalvanized ($\varepsilon = 0.7$) and galvanized ($\varepsilon = 0.35$). The incoming flux \dot{q}_{hasemi} is the same for the two configurations, which does not capture the fact that reducing emissivity physically leads to less radiant heat absorbed in a solid. The outgoing flux, in contrast, accounts for the term ε and therefore will be larger for the material with larger emissivity (as the latter is able to re-radiate more heat to the far field as its temperature increases). The result is that the net heat flux on the boundary of the ungalvanized steel would be smaller than that of the galvanized steel. This contradicts the physics and erroneously leads to higher temperatures in galvanized steel members than in (otherwise identical) ungalvanized members.

This contradicts the physics and erroneously leads to higher temperatures in galvanized steel members than in (otherwise identical) ungalvanized members. A possible solution to circumvent this limitation is the

following [22]. First, an equivalent hot gas temperature can be estimated using Eq. (2), which equates the total incident heat flux from Hasemi's model to the incident heat flux from the equivalent hot gas temperature T_g . Next, these equivalent hot gas temperatures are applied as boundary conditions to the steel members, and heat transfer at the boundary is evaluated from convection and radiation taking into account the appropriate emissivity for galvanization. As the Hasemi incident flux varies with time, so do the equivalent hot gas temperatures. It is noted though that this method is not mentioned in the Eurocode and requires specific implementation.

$$\dot{q}_{hasemi} = 35 (T_g - T_{amb}) + 0.7 (T_g^4 - T_{amb}^4) \quad (2)$$

5 CONCLUSIONS

This study focuses on the temperatures reached in steel framing members subjected to open car park fire scenarios. A parametric study was carried out considering the influence of the steel profiles, layout and number of burning vehicles, galvanization of the steel, and the modelling approaches adopted. The following conclusions are drawn:

- When subject to localised open car park fire, galvanization has the effect of delayed heating and reduced peak temperature. The peak temperatures in the investigated steel beam profiles are reduced by more than 50 °C under a scenario with a single burning car. However, this effect is reduced when subjected to localised fires with multiple burning vehicles because the steel temperature largely exceeds the melting temperature of the galvanization. As temperature rise in the steel members is also delayed owing to the galvanization, the member critical temperature may be reached a few minutes later when the member is galvanized.
- In terms of modelling approach, the Hasemi model is overconservative in predicting the temperatures in the steel beams at the ceiling level under open car park fires. This is mostly due to the assumption in the Hasemi model that flames are touching the ceiling during the whole fire duration, which contradicts observations from FDS modelling. While this study shows that applying Hasemi in open car park fire studies would be conservative, it could in fact be recommended to adopt more advanced modelling techniques (e.g., CFD-FEM) to complete the design based on a fire prediction that is not overly severe.
- Another limitation of the Hasemi model is that, since it provides an absorbed heat flux, it incorrectly predicts that reduced steel emissivity leads to higher steel temperatures. Indeed, the predicted absorbed heat flux in Hasemi is independent of the emissivity but the reemitted heat flux decreases with a reduction in emissivity. In general, the Hasemi model cannot capture the effect of different thermal properties on the absorbed heat flux. If engineers want to model the temperature elevation in galvanized steel structures, they need to adopt a model that can account for the modified emissivity, such as a CFD-FEM approach with a suitable steel thermal model.

Future works could focus on further improvements of simple fire models for open car parks. Specifically, a unified simple model predicting the heat flux received by the different members of the structure would facilitate analyses. The estimation of the heat flux should capture the effect of the thermal properties of the receiving surface, unlike the current version of the Hasemi model. An important challenge is for simple models to capture the transition between different phases of the fire-structure interaction, including when the structural member becomes engulfed in the flame.

ACKNOWLEDGMENT

The authors declare the following financial interests/personal relationships which may be considered as potential competing interests: Under a license agreement between Gesval S.A. and the Johns Hopkins University, Dr. Gernay and the University are entitled to royalty distributions related to the technology SAFIR described in the study discussed in this publication. This arrangement has been reviewed and approved by the Johns Hopkins University in accordance with its conflict of interest policies.

REFERENCES

- [1] F.S. of S.S. European Convention for Constructional Steelwork. Technical Committee 3, Fire Safety in Open Car Parks: Modern Fire Engineering, in: European Convention for Constructional Steelwork, 1993.
- [2] G. Heskestad, Engineering relations for fire plumes, *Fire Saf. J.* 7 (1984) 25–32.
- [3] A. Pchelintsev, Y. Hasemi, T. Wakamatsu, Y. Yokobayashi, Experimental and numerical study on the behaviour of a steel beam under ceiling exposed to a localized fire, *Fire Saf. Sci.* 5 (1997) 1153–1164.
- [4] N. Tondini, C. Thauvoys, F. Hanus, O. Vassart, Development of an analytical model to predict the radiative heat flux to a vertical element due to a localised fire, *Fire Saf. J.* 105 (2019) 227–243.
- [5] K. McGrattan, S. Hostikka, R. McDermott, J. Floyd, C. Weinschenk, K. Overholt, Fire dynamics simulator user's guide, NIST Spec. Publ. 1019 (2013).
- [6] B. Fettaf, *Fire Analysis of Car Park Building Structures*, (2016).
- [7] C. Fang, B.A. Izzuddin, R. Obiala, A.Y. Elghazouli, D.A. Nethercot, Robustness of multi-storey car parks under vehicle fire, *J. Constr. Steel Res.* 75 (2012) 72–84.
- [8] M. Somavilla, N. Tondini, Fire performance of a steel open car park in the light of the recent development of the localised fire model" LOCAFI", (2020).
- [9] O. Vassart, A. Morbioli, N. Tondini, J.-M. Franssen, S. Lechêne, An integrated modelling strategy between a CFD and an FE software, *J. Struct. Fire Eng.* 7 (2017) 217–233.
- [10] E. 1993-1-2, Eurocode 3: Design of Steel Structures - Part 1-2: General Rules – Structural Fire Design, European Committee for Standardization (CEN), Brussels, 2005.
- [11] B. Zhao, M. Roosefid, Guide pour la vérification du comportement au feu de parcs de stationnement largement ventilés en superstructure métallique, CTICM document (SRI – 11/110h– MR-BZ/NB), 2014.
- [12] J.B. Schleich, L.G. Cajot, J.M. Franssen, J. Kruppa, D. Joyeux, L. Twilt, J. Van Oerle, G. Aurtentxe, Development of design rules for steel structures subjected to natural fires in closed car parks (1997), EUR 18867EN, Rep. (1997).
- [13] J.-F. Cadorin, J.-M. Franssen, A tool to design steel elements submitted to compartment fires—OZone V2. Part 1: pre-and post-flashover compartment fire model, *Fire Saf. J.* 38 (2003) 395–427.
- [14] E. 1991-1-2, Eurocode 1: Actions on structures—Part 1-2: General actions—Actions on structures exposed to fire, Eur. Stand. (2002).
- [15] X. Yan, T. Gernay, Numerical modeling of localized fire exposures on structures using FDS-FEM and simple models, *Eng. Struct.* 246 (2021) 112997.
- [16] U. Wickström, D. Duthinh, K. McGrattan, Adiabatic surface temperature for calculating heat transfer to fire exposed structures, in: *Proc. Elev. Int. Interflam Conf. Intersci. Commun. London*, 2007.
- [17] U. Wickström, S. Hunt, B. Lattimer, J. Barnett, C. Beyler, Technical comment—Ten fundamental principles on defining and expressing thermal exposure as boundary conditions in fire safety engineering, *Fire Mater.* 42 (2018) 985–988.
- [18] M. Charlier, A. Glorieux, X. Dai, N. Alam, S. Welch, J. Anderson, O. Vassart, A. Nadjai, Travelling fire experiments in steel-framed structure: numerical investigations with CFD and FEM, *J. Struct. Fire Eng.* (2021).
- [19] X. Deckers, S. Haga, N. Tilley, B. Merci, Smoke control in case of fire in a large car park: CFD simulations of full-scale configurations, *Fire Saf. J.* 57 (2013) 22–34.
- [20] T. Gernay, P. Kotsovinos, *Advanced Analysis*, in: *Int. Handb. Struct. Fire Eng.*, Springer, 2021: pp. 413–467.
- [21] J.-M. Franssen, T. Gernay, Modeling structures in fire with SAFIR®: Theoretical background and capabilities, *J. Struct. Fire Eng.* (2017).
- [22] Zhao B., CTICM, email communication, Oct 6, 2022.